

more realistic conditions as long as ozone depletion by chlorine dominates in the Arctic.

It is important to note that ozone is only partially destroyed. In the Antarctic, where denitrification makes available a large amount of chlorine, almost complete destruction of ozone is observed. One would expect that the dilution effect here may not be as important as in the Arctic. We tested this by artificially increasing  $\alpha$  by a factor of 10 in our calculation to imitate the conditions prevailing in the Antarctic. Much higher depletion is then observed (Fig. 4b) but there is almost no sensitivity to dilution. This is not to say that mixing effects are absent. The relevant mechanism, not considered here, is the sensitivity of chlorine deactivation to the mixing of denitrified polar air with subtropical air<sup>8</sup> for which higher diffusivity or the lack of numerical resolution enhances the chemical reactivity.

We investigated whether the effect of small-scale inhomogeneities could be parametrized in low-resolution three-dimensional chemical models. A good fit to the curve of total ozone depletion for simulation E15 can be obtained by multiplying the corresponding curves for E30 and D1 respectively by a factor of 1.15 and by a factor of 1.37 (dashed curve with empty symbols in Fig. 4a) which is equivalent to increasing  $k_{\text{ClO}+\text{ClO}}$  in equation (1). In the case of chlorine deactivation, where chemical compounds are initially separated, Thuburn and Tan<sup>8</sup> propose decreasing the reaction rate in the model. The influence of dynamics on chemistry is complex so that designing robust parametrizations of small-scale

inhomogeneities might not prove an easy task. Meanwhile modellers should be aware that their results depend on the spatial resolution and that ultra-high-resolution modelling might be necessary to reach accurate results. □

Received 7 June; accepted 14 October 1996.

1. Webster, C. et al. *Science* **261**, 1130–1133 (1993).
2. Lefèvre, F. et al. *J. Geophys. Res.* **99**, 8183–8195 (1994).
3. Goutail, F. et al. in *Air Pollution Res. Rep.* No. 56 (eds Pyle, J. A., Harris, N. R. P. & Amanatidis, G. T.) 574–579 (European Communities, Brussels, 1996).
4. Goutail, F. et al. *J. Atmos. Chem.* (submitted).
5. Chipperfield, M. et al. *J. Atmos. Chem.* (submitted).
6. Holton, J. R. et al. *Rev. Geophys.* **33**, 403–436 (1995).
7. Edouard, S., Legras, B. & Zeitlin, V. *J. Geophys. Res.* **101**, 16771–16779 (1996).
8. Thuburn, J. & Tan, D. *J. Geophys. Res.* (submitted).
9. Haynes, P. H. & Anglade, J. *J. Atmos. Sci.* (in the press).
10. Selmin, V. *Comput. Meth. Appl. Mech. Eng.* **102**, 107–138 (1993).
11. van Leer, B. *J. Comput. Phys.* **23**, 276–299 (1977).
12. Salawitch, R., Wofsy, S. & Gottlieb, E. *P. Science* **261**, 1146–1149 (1993).
13. Molina, M. J. & Molina, L. T. *J. Phys. Chem.* **91**, 433–436 (1987).
14. Molina, M. J., Tso, T., Molina, L. T. & Wang, F. *Science* **238**, 1253–1257 (1987).
15. DeMore, W. B. *NASA Tech. Rep.* 92–20 (Jet Propulsion Lab., Pasadena, 1992).
16. Brunet, G., Vautard, R., Legras, B. & Edouard, S. *Mon. Weath. Rev.* **123**, 1037–1058 (1995).
17. Haynes, P. H. & Ward, W. E. *J. Atmos. Sci.* **50**, 3431–3453 (1993).
18. Manney, G. et al. *Geophys. Res. Lett.* **23**, 85–88 (1996).
19. Donovan, D. et al. *Geophys. Res. Lett.* **22**, 3489–3492 (1996).
20. Chipperfield, M., Cariolle, D. & Simon, P. *Geophys. Res. Lett.* **21**, 1467–1470 (1994).
21. Brunet, G. et al. *Geophys. Res. Lett.* **22**, 2729–2732 (1995).
22. Pommereau, J. P. & Goutail, F. *Geophys. Res. Lett.* **15**, 891–893 (1988).

ACKNOWLEDGEMENTS. We thank P. Haynes for comments. Computations were performed using the resources provided by IBM at Institut Pierre-Simon Laplace and by Institut du Développement et des Ressources en Informatique Scientifique (IDRIS).

## Possible role of dust-induced regional warming in abrupt climate change during the last glacial period

Jonathan Overpeck\*†, David Rind‡, Andrew Lacis‡ & Richard Healy§

\* NOAA Paleoclimatology Program, National Geophysical Data Center, 325 Broadway, E/GC, Boulder, Colorado 80303, USA

† Institute of Arctic and Alpine Research and Department of Geological Sciences, University of Colorado, Boulder, Colorado 80309, USA

‡ NASA Goddard Institute for Space Studies, 2880 Broadway, New York, New York 10025, USA

§ Center for Climate Systems Research, Columbia University, New York, New York 10027, USA

RECORDS from loess, sediments and ice cores indicate that the concentrations of tropospheric aerosols were higher in glacial periods than they are today, and that they peaked just before glacial terminations<sup>1–10</sup>. Energy-balance models have suggested<sup>11–14</sup> that these high glacial aerosol loadings were a source of glacial cooling of the order of 1–3 °C. Here we present a different view based on three-dimensional climate simulations, which suggest that high glacial dust loading may have caused significant, episodic regional warming of over 5 °C downwind of major Asian and ice-margin dust sources. Less warming was likely close to and over the oceans because of local cooling by sea-salt and marine sulphate aerosols. Abrupt changes in dust loading are associated with the Dansgaard–Oeschger and Heinrich climate events and with glacial termination<sup>3,8,15</sup>, suggesting that dust-induced warming may have played a role in triggering these large shifts in Pleistocene climate.

To examine the potential role of tropospheric dust in glacial climates, we carried out two sets of simulations with the NASA Goddard Institute for Space Studies (GISS) general circulation

model (Model II, using 4° × 5° latitude–longitude resolution, full seasonal cycle, interactive land surface and clouds<sup>16,17</sup>). First, two five-year simulations (with fixed sea surface temperature, SST) were run with identical late glacial conditions<sup>18</sup> but with different atmospheric dust loadings. In the ‘modern-dust’ simulation, we used present-day monthly mean dust<sup>19</sup> as shown in Fig. 1a, b). In the ‘glacial-dust’ simulation, average modern-day desert silt and clay mineral dust<sup>19,20</sup> was prescribed with peak abundance in the lower troposphere over each 4° × 5° model grid box containing some fraction of the North American ice sheet or desert (Fig. 1c). The optical depth of glacial dust was specified to be 0.168, in accordance with ice-core observations<sup>1,7</sup>, distributed uniformly over the affected grid boxes.

Comparing ‘glacial-dust’ with ‘modern-dust’ simulations shows warming patterns (Fig. 2a) that differ substantially from the pattern of applied radiative forcing (Fig. 1c); this points to the importance of regional differences in feedback interactions that arise from changes in static stability due to solar heating and longwave heating/cooling by dust aerosols<sup>19,20</sup>. This behaviour differs from the classical response inferred from changes in energy balance arising from aerosol effects on planetary albedo<sup>21,22</sup>. Except for regions of northern Canada and Alaska, the dust-induced average annual warming was greater at progressively higher latitudes, and was greatest (up to 4.4 °C) in regions with dust over high-albedo snow- and ice-covered areas. Because the SSTs were fixed in these simulations, the global temperature change was small. Contributing changes in cloud cover, atmospheric water vapour, and surface albedo are listed in Table 1.

Our results are consistent with recent assessments of how mineral dust affects present climate<sup>19,20</sup>. Decreased backscattering of incident solar radiation occurs when the aerosol overlies high-albedo snow- or ice-covered surfaces, whereas solar backscattering is increased when the dust overlies dark land and ocean surfaces. The effective cloud single scattering albedo decreases when dust occurs within clouds<sup>19</sup>. In addition to its shortwave effect, dust loading also contributes a small, but significant, amount of greenhouse warming through increased absorption of thermal radiation<sup>17</sup>. Within this general context, specific causes of surface warming varied from region to region. Typically, regions with reduced planetary albedo are associated with increased solar

heating of the troposphere and surface. Some of the warming resulted from tropospheric trapping of thermal radiation. In addition, changes in atmospheric pressure and circulation patterns were evident, indicating that some of the warming arose from warm air being advected from the south and from warmer ocean areas.

These simulations with fixed SSTs were intended to focus on the regional sensitivity of the direct radiative effects of mineral dust aerosols. The overall global response was limited by the fixed SSTs, but the negative net radiation at the top of the atmosphere (Table 1) implies global radiative disequilibrium such that the globe would cool if the SSTs were allowed to adjust.

A more complete test of model sensitivity to mineral dust is provided by our second set of GCM simulations which are identical to the first set but with interactive SSTs. These simulations were run to full equilibrium (75 years) using ocean heat transports calculated from the fixed-SST 'modern-dust' simulation. Here, North Atlantic heat transports implied in the fixed-SST 'glacial-dust' simulation were not significantly different from today's, although to have maintained the Pacific and global SSTs under late glacial conditions would have required increasing peak transports by 18 and 6%, respectively.

Surface air temperatures obtained with interactive SSTs are only slightly cooler than those with fixed SSTs, with differences occurring primarily over land. Several of the feedbacks changed sign and thus mitigated the temperature changes. In particular, low cloud cover decreased, and the planetary albedo change became negative. Overall, the more realistic interactive-SST ocean reduced the amount of mid- to high-latitude warming from 4.4 °C (Fig. 2a) to 2.4 °C (Fig. 2b), but the principal regions of significant warming remain concentrated in areas where the dust loading coincides with snow- or ice-covered land surfaces.

Some aspects of our simulations may have underestimated the full potential of regional dust-induced warming. First, although

TABLE 1 Regional annual-average global climate anomalies

	Fixed SSTs	Interactive SSTs
Surface air temperature (°C)	0.19	0.13
Peak warming over land (°C)	4.40	2.40
Net radiation at top of atmosphere*†	-0.40	0.00
Planetary albedo†	0.09	-0.08
Ground albedo†	-0.32	-0.09
Atmospheric water vapour (mm)	0.30	0.10
Total cloud cover (%)	0.40	0.00
High cloud (%)	-0.10	0.10
Low cloud (%)	0.70	-0.20

These anomalies are for our 'glacial-dust' minus 'modern-dust' simulations (see text).

\* Negative value implies atmospheric disequilibrium.

† All radiation terms in  $W m^{-2}$ .

the magnitude of our dust loading was similar to Greenland ice-core estimates, these ice cores were far from hypothesized Asian desert and North American ice-margin dust sources<sup>1,7,23,24</sup>. True loadings were probably much higher closer to these source regions. Second, modern studies highlight the regional and episodic nature of major aerosol loadings<sup>25,26</sup>, and make it clear that dust-induced climate changes could have been regionally much more intense than those implied by our simulations with modest levels of uniform optical depth. Also, we did not include the reduction of snow albedo by dust, an unknown but potentially important factor which would serve to amplify the warming. Last, we did not include microphysical aerosol-cloud interactions that could have altered cloud extent and cloud optical properties<sup>27,28</sup>.

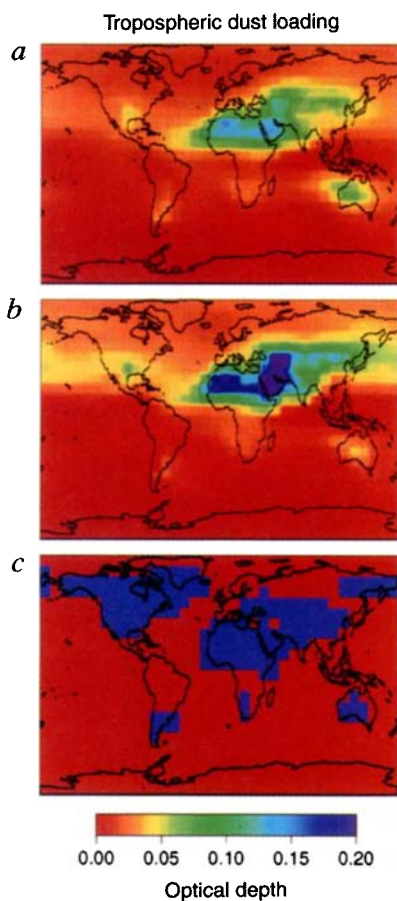


FIG. 1 Dust loading prescribed in the climate model experiments. Different monthly modern dust loadings (a, annual average; b, June average) were prescribed using observed optical depths<sup>17,19</sup>; in contrast the same dust loading was prescribed for each month of the glacial simulations (c). Prescribed regional glacial dust loadings in the Northern Hemisphere are in accordance with time-averaged observations<sup>1,7</sup>; it is likely that episodic peak glacial loadings may have been significantly greater than those we used.

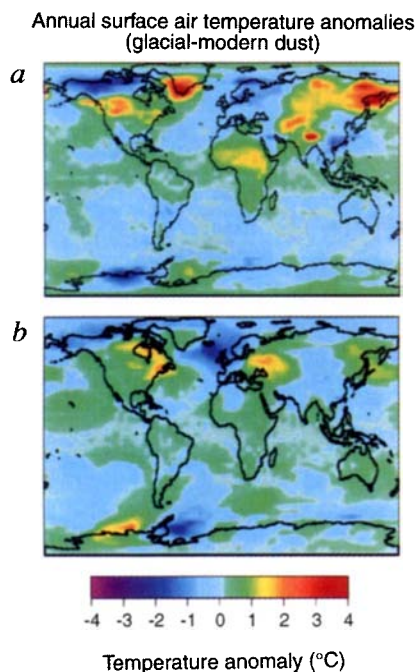


FIG. 2 Simulated annual surface air temperature anomalies between the 'glacial-dust' and 'modern-dust' simulations. Two sets of experiments were carried out, one with fixed sea surface temperatures (a), and the other with interactive sea surface temperatures (b). Both sets show significant warming in areas of glacial tropospheric dust loading. Peak dust loading, and hence warming, was probably significantly greater than shown here (see text).

Here we have simulated the effects of dust aerosol only. For a more complete study, other aerosols would need to be considered<sup>12,26</sup>. In particular, tropospheric sea-salt concentrations were as high as one-third of the total dust loading in some marine and coastal locations<sup>7,8</sup>. But rapid fall-off of sea-salt concentration inland from ocean sources due to the typically large size of salt particles make it less likely that sea salt could have achieved continental distributions nearly as significant as the mineral dust<sup>29</sup>. Also, glacial marine sulphate loadings were significantly higher in Southern Hemisphere polar regions compared to present, but smaller in the Northern Hemisphere, unlike the situation with dust<sup>8,30</sup>. Carbon/soot concentrations also appear to have been negligible during glacial periods<sup>31</sup>. Thus, mineral dust appears to have been the most globally distributed aerosol, with the largest

radiative effect over snow- and ice-covered regions.

Tropospheric dust loading would be expected to increase steadily with the extent of glaciation. Thus, winds, dust sources, and hence dust entrainment would have been largest along the margins of ice sheets<sup>14</sup>. Peak Asian dust (loess) loading also coincided with the strong winds and minimal monsoon precipitation associated with glaciation<sup>15,32</sup>. These are the same areas where dust would have produced significant warming once the dust sources were sufficiently developed. Greenland ice-core data suggest that dust loading, mostly of Asian origin<sup>23</sup>, peaked just before the well-known Dansgaard-Oeschger warm events<sup>3</sup>, before and during Heinrich events<sup>8</sup>, and just before glacial terminations<sup>2,3,5,7</sup>.

Most recent investigations of these abrupt Pleistocene events, including those that have coupled ice-core events to major shifts in North Atlantic SSTs and regional circulation, indicate that large-scale forcing is needed to explain the simultaneous effect on several different ice sheets<sup>33</sup>. Episodic dust loading may have provided the warming needed to trigger the ice, ocean and atmospheric changes associated with these events. Dust loading and associated snow darkening are leading mechanisms for explaining the abrupt termination of the 100-kyr glacial cycle<sup>34</sup>. The initiation of Heinrich events required some climatic or climate-induced sea-level trigger (for example, dust-induced warming) to decouple ice sheets from their beds and generate the moderate (Dansgaard-Oeschger) or massive (Heinrich) meltwater/iceberg discharges from several different Northern Hemisphere ice sheets<sup>33,35</sup>.

Warming following these events would have led to the formation of extensive lakes which would have trapped dust-sized sediment entrained in outwash<sup>14</sup>. At the same time, hemispheric warming following the Heinrich events<sup>15</sup> would have reduced Tibetan plateau snow cover, increased heating of land in summer, strengthened the Asian monsoon, and stabilized dust sources with higher precipitation<sup>36</sup>. Thus, peak dust loading may have triggered the same climate changes that then led to observed abrupt decreases in dust loading<sup>3,7,8,15</sup>.

Our results point to dust aerosols as a potential source of episodic warming during the last glacial period, and suggest that this warming might be the trigger mechanism needed to account for previously unexplained major abrupt climate events. Our study also highlights the complicated nature of modelling aerosol-induced climate change, and the need for three-dimensional general circulation model simulations to model all aspects of the climate response, particularly at high latitudes with absorbing aerosols and under cloudy sky conditions. New ice-core and geological data are needed to improve our understanding of aerosol characteristics, their sources and transport processes during the Pleistocene. Only then will it be possible to extend our modelling approach to refine the exact magnitude of past dust-induced warming. □

Received 15 January; accepted 17 October 1996.

- Thompson, L. & Mosley-Thompson, E. *Science* **212**, 812–815 (1981).
- Petit, J. R., Briat, M. & Royer, A. *Nature* **293**, 139–194 (1981).
- Hammer, C. U. et al. in *Greenland Ice Core: Geophysics, Geochemistry, and the Environment* (eds Langway, C. C. Jr, Oeschger, H. & Dansgaard, W.) 90–94 (Geophys. Monogr. 33, Geophys. Union, Washington, 1985).
- Pye, K. *Aeolian Dust and Dust Deposits* (Academic, London, 1987).
- De Angelis, M., Barkov, N. I. & Petrov, V. N. *Nature* **325**, 318–321 (1987).
- Delmas, R. J. & Legrand, M. in *The Environmental Record in Glaciers and Ice Sheets* (eds Oeschger, H. & Langway, C. C.) 319–341 (Wiley, New York, 1989).
- Hansson, M. E. *Tellus* **46B**, 390–418 (1994).
- Mayewski, P. A. et al. *Science* **263**, 1747–1751 (1994).
- Rea, D. *Rev. Geophys.* **32**, 159–195 (1994).
- Thompson, L. et al. *Science* **269**, 46–50 (1995).
- Harvey, L. D. *Nature* **334**, 333–335 (1988).
- Anderson, T. L. & Charlson, R. J. *Nature* **345**, 393 (1990).
- Crowley, T. J. & North, G. R. *Paleoclimatology* (Oxford, Univ. Press, New York, 1991).
- Hughes, T. *Palaeogeogr. Palaeoclimatol. Palaeoecol.* **97**, 203–234 (1992).
- Porter, S. C. & An, Z. *Nature* **375**, 305–308 (1995).
- Hansen, J. et al. *Mon. Weath. Rev.* **3**, 609–662 (1983).
- Lacis, A. A. & Mischenko, M. I. in *Aerosol Forcing of Climate* (eds Charlson, R. J. & Heintzenberg, J.) 11–42 (Wiley, New York, 1995).
- Rind, D. et al. *Clim. Dyn.* **1**, 3–33 (1986).
- Tegen, I., Lacis, A. A. & Fung, I. *Nature* **380**, 419–422 (1996).
- Tegen I. & Lacis, A. A. *J. Geophys. Res.* **101**, 19237–19244 (1996).

- Chylek, P. & Coakley, J. A. *Jr Science* **183**, 75–77 (1974).
- Coakley, J. A. Jr & Chylek, P. *J. Atmos. Sci.* **32**, 409–418 (1975).
- Biscaye, P. E. et al. *Eos (Spring Mtg suppl.)* **77**, 157 (1996).
- Frenzel, B., Pécsi, M. & Velichko, A. A. (eds) *Atlas of Paleoclimates and Paleoenvironments of the Northern Hemisphere, Late Pleistocene-Holocene* (Gustav-Fischer, Stuttgart, 1992).
- Tegen, I. & Fung, I. *J. Geophys. Res.* **99**, 22897–22914 (1994).
- Li, X., Maring, H., Savoie, D., Voss, K. & Prospero, J. M. *Nature* **380**, 416–419 (1996).
- Curry, J. A. et al. *J. Clim.* **9**, 1731–1764 (1996).
- Curry, J. A. *Sci. Total Environ.* **160/161**, 777–791 (1995).
- Mulvaney, R. & Wolff, E. W. *Ann. Glaciol.* **20**, 440–447 (1994).
- Hansson, M. E. & Saitzman, E. S. *Geophys. Res. Lett.* **20**, 1163–1166 (1993).
- Chylek, P., Johnson, B. & Wu, H. *Ann. Geophys.* **10**, 625–629 (1992).
- Liu, T. S. et al. *Loess and the Environment* (China Ocean, Beijing, 1985).
- Bond, G. C. & Lotti, R. *Science* **267**, 1005–1010 (1995).
- Peltier, W. R. et al. in *Global Changes in the Perspective of the Past* (eds Eddy, J. A. & Oeschger, H.) 239–262 (Wiley, New York, 1993).
- MacAyeal, D. R. *Paleoceanography* **8**, 775–784 (1993).
- Overpeck, J. T., Anderson, D., Trumbore, S. & Prell, W. *Clim. Dynam.* **12**, 213–225 (1996).

ACKNOWLEDGEMENTS. We thank J. Curry, K. Kreutz, D. MacAyeal, P. Mayewski, E. Steig, I. Tegen, S. Porter, S. Thompson, L. Thompson and R. S. Webb for discussions and comments. This work was supported by the Climate Dynamics Program of the US NSF, the NOAA Paleoclimatology Program and NASA.

CORRESPONDENCE should be addressed to J.O. at the National Geophysical Data Center (e-mail: jto@ngdc.noaa.gov).